Real squashing mode in textures in ^{3}He-B

V. P. Mineev

L. D. Landau Institute of Theoretical Physics, Academy of Sciences of the USSR
(Submitted 16 July 1984)
Zh. Eksp. Teor. Fiz. **88**, 507–515 (February 1985)

The shape of the line of ultrasonic absorption due to the various components of the real squashing mode in textures in ^{3}He-B is analyzed. The additional splitting of the absorption line for the $M = 0$ component of the real squashing mode in a magnetic field is explained. The absence of such a splitting for the lines with $M = \pm 1, \pm 2$ in a planar geometry is also explained. Structural features in the lines of ultrasonic absorption by various components of the real squashing mode in a rotating cylindrical vessel holding ^{3}He-B are discussed.

1. INTENSITY OF ULTRASOUND ABSORPTION BY THE REAL SQUASHING MODE BETWEEN TWO PARALLEL PLATES

The collective modes in superfluid ^{3}He-B are oscillations of the order parameter about the equilibrium value

$$A_{\alpha i}^0=\Delta R_{\alpha i}e^{i\Phi},$$

which are coupled with oscillations of the particle distribution function. Here Δ is the temperature-dependent modulus of the order parameter, $R_{\alpha i}$ is an orthogonal matrix ($i = 1, 2, 3$ is the orbital index, and $\alpha = 1, 2, 3$ is the spin index), and $\exp(i\Phi)$ is a phase factor. In the case of p pairing (the spin of the pair is $S = 1$, and the orbital angular momentum of the pair is $L = 1$), the order parameter is generally a complex 3×3 matrix $A_{\alpha i}$ specified by 18 real parameters, whose number determines the number of independent collective modes. The modes are by convention classified[1] with the help of quantum numbers which are the eigenvalues of the following operators: the square of the total angular momentum $J_i = L_i + R_{\alpha i}S_\alpha$, the projection ($M$) of J_z onto a direction ($\hat{\mathbf{z}}$) which we single out, and the parity of T under complex conjugation. The operator J_i is the sum of the operator representing the orbital angular momentum, L_i, and of the operator representing the spin, $R_{\alpha i}S_\alpha$, in a coordinate system whose spin unit vectors $\hat{x}_\alpha$ are rotated from those of the orbital system, x_i, by the orthogonal matrix: $\hat{x}_\alpha = R_{\alpha i}\hat{x}$. The equilibrium state of the liquid is characterized by the quantum number $J = 0$; i.e., $J_l A^0_{\alpha i} = 0$. There are accordingly two ($T = \pm 1$) modes with $J = 0$, two triply degenerate modes with $J = 1$ ($M = 0, \pm 1$), and two fivefold-degenerate modes with $J = 2$ ($M = 0, \pm 1, \pm 2$).

The collective modes in ^{3}He-B are seen as peaks in the absorption of ultrasound at frequencies corresponding to the various modes (see the review by Ketterson *et al.*[2] and the bibliography there). The greatest progress has come in research on the "real quadrupole mode" or "real squashing mode,"[3] which has the quantum numbers $J = 2$ and $T = 1$. Its frequency is $\omega = \omega_0 = (8/5)^{1/2}\Delta(T)$, if we ignore Fermi-liquid corrections. This mode is an oscillation of the spin distribution function and is thus weakly coupled (the strength of the coupling depends on the asymmetry in the distribution of particles and holes) to ultrasound with quantum numbers $J = 0$, $T = -1$. It thus becomes possible to observe[4] the fivefold splitting of the real squashing mode in a magnetic field H, as predicted theoretically by Tewordt and Schopohl[5]:

$$\omega=\omega_M=\omega_0+Mg(T)\omega_L \tag{1}$$

[$g(T)$ is an effective g-factor, ω_L is the Larmor frequency, and $\omega_L = \gamma H$ if Fermi-liquid effects are ignored]. It is also possible to observe a dispersive splitting of the squashing mode in a zero field.[6]

The dispersion relations for the various components of the real squashing mode,

$$\begin{aligned} &M=0:\ \omega^2=\omega_0^2+0{,}44v_F^2q^2;\\ &M=\pm1:\ \omega^2=\omega_0^2+0.39v_F^2q^2;\\ &M=\pm2:\ \omega^2=\omega_0^2+0{.}22v_F^2q^2 \end{aligned} \tag{2}$$

($\mathbf{q}$ is the wave vector, and v_F is the Fermi velocity), and the dispersion relations for all the other collective modes in ^{3}He-B were first derived in a pioneering but unnoticed paper by Vdovin[7] back in 1961 (!); these relations have since been rederived by several authors.[1,8–12]

Recent experiments[6] in comparatively strong fields, $H > 500$ G, have also revealed an additional twofold splitting of the central component of the real squashing mode ($M = 0$). This splitting has been explained theoretically by Volovik (Ref. 13; see Ref. 14 for more details). It has been shown that the frequency of the real squashing mode depends on the texture of the order parameter $R_{\alpha i}$:

$$\omega^2=\omega_M^2+c_1^2q^2+c_2^2q^2(\hat{\mathbf{q}}\hat{\mathbf{h}})^2. \tag{3}$$

Expression (3) holds under the approximation[14] $c_2^2q^2/\omega \ll \omega_L g \ll \omega_0$. Here c_1 and c_2 are the sound velocities; $\hat{\mathbf{q}} = \mathbf{q}/q$ is a unit vector along the sound propagation direction; $\hat{h}_i = R_{\alpha i}H_\alpha/H$ is a unit vector along the quantization axis for the total angular momentum J_i; and $R_{\alpha i}$ is the three-dimensional rotation matrix, which specifies the order parameter in ^{3}He-B. The matrix $R_{\alpha i}$ is customarily parametrized by means of the unit vector ($\hat{\mathbf{n}}$) along the rotation axis and the rotation angle θ, which is fixed by the spin–orbit interaction: $\theta = \theta_0 = \arccos(-1/4)$, so that

$$R_{\alpha i}={}^1/_4(-\delta_{\alpha i}+5\hat{n}_\alpha\hat{n}_i-15^{1/2}e_{\alpha il}\hat{n}_l). \tag{4}$$

In the experiments of Ref. 6, the sound propated through ^{3}He-B between two parallel plane plates separated by a distance $l = 4$ mm; the vector $\hat{\mathbf{q}}$ was along $\hat{\mathbf{\nu}}$ (the unit normal to the plates); and the magnetic field $\mathbf{H}$ was parallel to the plane of the plates. In fields strong enough that the distance between the plates exceeds the magnetic length ξ_H, by virtue of the orienting effect of the magnetic-anisotropy energy (see Ref. 15, for example)

 0038-5646/85/020297-05$04.00

$$F_H=-a\int(\hat{\mathbf{n}}\mathbf{H})^2\,dV=-\frac{4}{5}aH\int dV(\mathbf{H}\hat{\mathbf{h}}),\tag{5}$$

the vector $\hat{\mathbf{h}}$ is parallel to the field $\mathbf{H}$ at a distance greater than ξ_H from the plates, while at the surfaces of the plates it is parallel to $\pm\hat{\mathbf{v}}$ by virtue of the orienting effect of the surface energy

$$F_S=-d\int dS(\hat{v}_iR_{\alpha i}H_\alpha)^2=-dH^2\int dS(\hat{\mathbf{v}}\hat{\mathbf{h}})^2\tag{6}$$

(d is a constant). Figure 1 (see Ref. 13) shows the distribution of $\hat{\mathbf{h}}$ in the volume between the plates. This distribution can be described by the simple expression ($\bar{\mathbf{v}}\|\mathbf{z}$)

$$\hat{\mathbf{h}}=\hat{\mathbf{v}}\cos\gamma(z)+(\mathbf{H}/H)\sin\gamma(z).\tag{7}$$

Here we have $\gamma(\pm l/2)=0$ at the plate surfaces and $\gamma(0)=\pi/2$ in the plane halfway between the plates. The frequency of the real squashing mode thus turns out to depend on the texture:

$$\omega^2=\omega_M{}^2+c_1{}^2q^2+c_2{}^2q^2\cos^2\gamma(z).\tag{8}$$

The ultrasonic wavelength $q^{-1}\sim10^{-4}=10^{-5}$ cm is much shorter than the magnetic length ξ_H, over which the direction of $\hat{\mathbf{h}}$ changes. We can thus use the approximation of local oscillators, according to which there is an independent real squashing mode, with a frequency determined by (8), at each point in the vessel. The damping of the ultrasound due to the excitation of the real squashing mode is proportional to the spectral density

$$P(\omega)=\frac{1}{l}\int_{-l/2}^{l/2}\delta(\omega-\omega(z))\,dz=\left|l\frac{\partial\omega}{\partial z}\right|^{-1}_{z=z(\omega)},\tag{9}$$

which tends toward infinity at the two points $\omega^2=\Omega_1^2=\omega_M^2+c_1^2q^2$ (the absorption component due to the central part of the vessel) and $\omega^2=\Omega_2^2=\omega_M^2+c_1^2q^2+c_2^2q^2$ (the absorption component due to the region near the plates) in accordance with

$$P(\omega\to\Omega_{1,2})\propto(2\Omega_{1,2})^{1/2}/2lc_2q|\gamma_{1,2}'|\,|\omega-\Omega_{1,2}|^{1/2},\tag{10}$$

$$\gamma_1'=\partial\gamma/\partial z|_{z=0},\qquad \gamma_2'=\partial\gamma/\partial z|_{z=\pm l/2}.$$

To calculate the exact values of the derivatives we need to find the spatial texture of the vector $\hat{\mathbf{n}}$ (as discussed below). In sufficiently strong magnetic fields there is thus a texture-induced splitting of the ultrasonic absorption line corresponding to the real squashing mode with $M=0$ (Ref. 13). The magnitude of the splitting is independent of the field in strong fields and is given by

$$\Delta\omega=\Omega_2-\Omega_1=c_2{}^2q^2/2\omega_0.$$

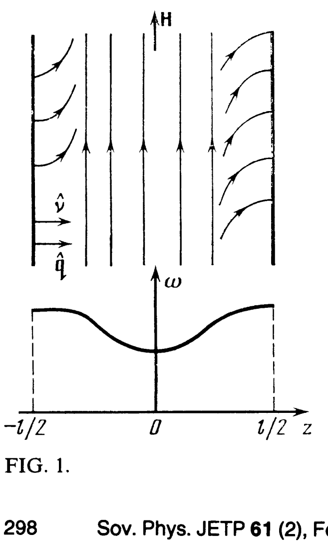

FIG. 1.

It is important to note that dispersion relation (8) holds for any component of the real squashing mode (with $M=0$, ±1, ±2), although the constants ω_M, c_1, and c_2 have of course different values for the different components. The frequency ω_M is determined by (1). Comparison of the expressions given by Volovik and Khazan[14] with Vdovin's results, (2), yields

$$M=0:\quad c_1{}^2=0.28v_F{}^2,\quad c_2{}^2=0.17v_F{}^2;$$
$$M=\pm1:\quad c_1{}^2=0.3v_F{}^2,\quad c_2{}^2=0.08v_F{}^2;$$
$$M=\pm2:\quad c_1{}^2=0.39v_F{}^2,\quad c_2{}^2=-0.17v_F{}^2.$$

We must therefore examine why experiments reveal a splitting of only the $M=0$ component. A natural explanation arises when we note that the constant (λ_M) of the interaction between the ultrasound and the real squashing mode depends also on the texture of the order parameter $R_{\alpha i}$. According to Ref. 16, λ_M is small to the extent that the asymmetry in the distributions of the particles and holes is small, and it differs for the components of the real squashing mode with different values of M:

$$\lambda_M\propto P_{2M}{}^2(\gamma).\tag{11}$$

Here P_{2M} are the associated Legendre polynomials, and γ is the angle (introduced earlier) between $\hat{\mathbf{q}}$ and the quantization axis $\hat{\mathbf{h}}$: $\cos\gamma=\hat{\mathbf{q}}\hat{\mathbf{h}}$. The squares of the associated Legendre polynomials are written as functions of $\cos^2\gamma$:

$$\begin{aligned}P_{20}{}^2(\cos^2\gamma)&={}^1/_4(1-3\cos^2\gamma)^2,\\ P_{21}{}^2(\cos^2\gamma)&={}^3/_2(1-\cos^2\gamma)\cos^2\gamma,\\ P_{22}{}^2(\cos^2\gamma)&={}^3/_8(1-\cos^2\gamma)^2.\end{aligned}\tag{12}$$

To derive the intensity of the ultrasound absorption due to the excitation of the various components of the real squashing mode in the texture, we must thus integrate the frequency distribution $\delta(\omega-\omega(z))$ with a weight $\lambda_M(z)$:

$$I_M(\omega)\propto\frac{1}{l}\int_{-l/2}^{l/2}\delta(\omega-\omega(z))P_{2M}{}^2(\cos^2\gamma)\,dz$$

$$=P(\omega)P_{2M}{}^2\left(\frac{\omega^2-\Omega_1{}^2}{c_2{}^2q^2}\right).\tag{13}$$

The spectral density $P(\omega)$ in (9) has square-root singularities [see (10)] at the points $\omega=\Omega_1,\ \Omega_2$, but only for $M=0$ do these singularities cause a splitting of the absorption line. The reason for this situation lies in the zeros of the Legendre polynomials. In the case $M=\pm1$, they are at the same points, $\omega=\Omega_1,\ \Omega_2$ ($\gamma=0,\ \pi/2$), while in the case $M=\pm2$ they are at the point $\omega=\Omega_2$ ($\gamma=0$).

We thus find the following behavior of the ultrasonic absorption intensity near the singular points of the spectral density:

$$I_0(\omega\to\Omega_1)\propto(2\Omega_1)^{1/2}/8lc_2q|\gamma_1'|(\omega-\Omega_1)^{1/2},\tag{14a}$$

$$I_0(\omega\to\Omega_2)\propto(2\Omega_2)^{1/2}/2lc_2q|\gamma_2'|(\Omega_2-\omega)^{1/2},\tag{14b}$$

$$I_{\pm1}(\omega\to\Omega_{1,2})\propto3(2\Omega_{1,2})^{3/2}|\omega-\Omega_{1,2}|^{1/2}/4l(c_2q)^3|\gamma_{1,2}'|,\tag{15}$$

$$I_{\pm2}(\omega\to\Omega_1)\propto 3(2\Omega_1)^{1/2}/16l|c_2|q|\gamma_1'|(\omega-\Omega_1)^{1/2}, \qquad (16a)$$

$$I_{\pm2}(\omega\to\Omega_2)\propto(2\Omega_2)^{5/2}(\Omega_2-\omega)^{3/2}/l(|c_2|q)^5|\gamma_2'|. \qquad (16b)$$

We also note that the absorption (I_0) for the $M=0$ component vanishes at

$$\omega=\Omega_{min}=({}^2/{}_3\Omega_1^2+{}^1/{}_3\Omega_2^2)^{1/2}$$

(the zero of the Legendre polynomial P_{20}). There is thus in fact a splitting of the $M=0$ line. The intensity ($I_\pm$) of the absorption for the $M=\pm1$ component vanishes at the boundaries of the absorption interval, $\omega=\Omega_{1,2}$, and it reaches a maximum at the intermediate point $\omega=(\Omega_1\Omega_2)^{1/2}$. Finally, $I_{\pm2}$ tends toward infinity at the lower boundary, $\omega=\Omega_1$, and vanishes at $\omega=\Omega_2$. We recall that the values of ω_M, c_1, c_2, Ω_1, and Ω_2 are different for the components with the different values of M.

We have thus found a qualitative description of the shape of the ultrasonic absorption lines corresponding to the components of the real squashing mode for a planar geometry and for a rather strong magnetic field, directed parallel to the surfaces of the plates. In this case there is a texture-induced splitting of only the central ($M=0$) peak. In the case of an oblique field it is possible to observe also a splitting of the ultrasonic absorption lines corresponding to other components of the real squashing mode. For an exact description of the shape of the absorption lines we need to find the texture of the vector $\hat{\mathbf{n}}$ in the volume between the plates. For weak fields, this texture has been found by Smith *et al.*[17] (see also Ref. 15). For fields of arbitrary magnitude and direction, this problem would obviously require numerical methods. In the case of a strong field ($\xi_H\ll l$) parallel to the surfaces of the plates, however, we can estimate the derivatives $(\partial\gamma/\partial z)_{1,2}$ near the singular points $\omega=\Omega_{1,2}$ of the spectral density $P(\omega)$ in a rather simple way.

Following Hakonen and Volovik,[18] we write the sum of the gradient energy and the magnetic-anisotropy energy (5) in the form

$$F=F_\nabla+F_M=\frac{16}{13}c\int_{-l/2}^{l/2}dz\left\{(\nabla_i\hat{\mathbf{n}})^2-\frac{1}{16}[5^{1/2}(\hat{\mathbf{n}}\operatorname{rot}\hat{\mathbf{n}})+3^{1/2}\operatorname{div}\hat{\mathbf{n}}]^2-(\xi_H')^{-2}(\hat{\mathbf{n}}\hat{\mathbf{x}})^2\right\}, \qquad (17)$$

$$\xi_H'=\xi_H({}^{16}/{}_{13})^{1/2},\quad \xi_H=(c/aH^2)^{1/2}, \qquad (18)$$

$$c=\frac{13}{64}\frac{\hbar^2}{m}\rho_s^0,\quad \rho_s^0=\frac{m}{m^*}(1-Y(T)), \qquad (19)$$

where $Y(T)$ is the Yoshida function. Here the $\hat{\mathbf{x}}$ axis is along the magnetic field $\mathbf{H}$ (Fig. 2), and the vector $\hat{\mathbf{n}}$ is written in terms of the angles θ and φ: $\hat{\mathbf{n}}=(\sin\theta\cos\varphi,\ \sin\theta\sin\varphi,\ \cos\theta)$. The surface energy in (6) is minimized when $\hat{\mathbf{n}}$ has the value

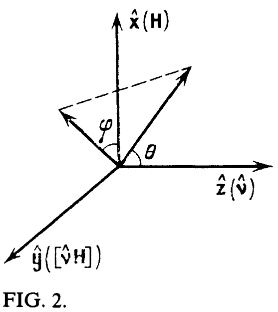

FIG. 2.

$$\hat{\mathbf{n}}(z=\pm l/2)=(5^{-1/2};\ ({}^3/{}_5)^{1/2};\ 5^{-1/2}). \qquad (20)$$

To find the texture of the vector $\hat{\mathbf{n}}$ we must solve Euler-Lagrange equations for the functional in (17) with boundary conditions (20). Far from the walls of the vessel, i.e., at distances $|\pm l/2-z|\gg\xi_H$, where $\theta\to\pi/2$, $\varphi\to0$, a solution of the linearized equations yields

$$\theta=\pi/2+A_1\operatorname{sh}(z/\xi_H')+A_2\operatorname{sh}(2^{1/2}z/\xi_H'),$$
$$\varphi=-({}^3/{}_5)^{1/2}A_1\operatorname{sh}(z/\xi_H')+({}^5/{}_3)^{1/2}A_2\operatorname{sh}(2^{1/2}z/\xi_H'). \qquad (21)$$

Using (4), we can then find the behavior $\cos\gamma(z)=\hat{z}_iR_{\alpha i}\hat{\mathbf{X}}_{\hat\alpha}$ at $|z|\ll\xi_H'$, in which we are interested:

$$\gamma(z)\approx\pi/2+2A_1(z/\xi_H'). \qquad (22)$$

To find the constant A_1 we must join solutions (21) at intermediate distances, $|z|\gg\xi_H$ and $|\pm l/2-z|\gg\xi_H$, with the solutions of the nonlinear Euler-Lagrange equations satisfying boundary conditions (20). Using the results of Ref. 18, we find

$$\gamma_1'=\left.\frac{\partial\gamma}{\partial z}\right|_{z=0}=\frac{2{,}2({}^5/{}_2)^{1/2}}{\xi_H'}\exp\left(-\frac{l}{2\xi_H'}\right). \qquad (23)$$

As for the derivative γ_2', we note that in the absence of numerical calculations we can at best assign it an order of magnitude:

$$\gamma_2'=\left.\frac{\partial\gamma}{\partial z}\right|_{z=\pm l/2}\sim\frac{1}{\xi_H}. \qquad (24)$$

The quantity ξ_H depends on the field, the temperature, and the pressure. For $P=29.4$ bar, for example, we have, according to Ref. 18,

$$\xi_H[\mathrm{cm}]=40\left(1-\frac{T}{T_c}\right)\Big/H[\mathrm{G}].$$

Expressions (23) and (24) differ by an exponentially small factor. Consequently, as the field or the temperature is increased the intensity of the left-hand ultrasonic absorption peak $I_0(\omega\to\Omega_1)$ should become greater than that of the right-hand peak $I_0(\omega\to\Omega_2)$, according to (14a) and (14b).

2. REAL SQUASHING MODE IN ^{3}He-B IN A ROTATING CYCLINDER

Let us examine the absorption of ultrasound by the real squashing mode in a rotating cylinder with ^{3}He-B. For simplicity we restrict the discussion to the case in which the angular velocity Ω, the magnetic field $\mathbf{H}$, and the sound propagation direction $\hat{\mathbf{q}}$ are parallel to each other and directed along the axis ($\hat{\mathbf{z}}$) of the cylinder. Writing the vector $\hat{\mathbf{n}}$ in polar coordinates as $\hat{\mathbf{n}}=(\cos\alpha\sin\beta,\ \sin\alpha\sin\beta,\ \cos\beta)$, we find

$$\cos\gamma(\mathbf{r})=\hat{q}_iR_{\alpha i}H_\alpha/H={}^1/{}_4[-1+5\cos^2\beta(\mathbf{r})], \qquad (25)$$

where r is the distance from the axis of the cylinder. In the case of axisymmetric textures, the lines of constant frequency, $\omega(\mathbf{r})=\text{const}$,

$$\omega^2(\mathbf{r})=\omega_M{}^2+c_1{}^2q^2+c_2{}^2q^2\cos^2\gamma(\mathbf{r}), \qquad (26)$$

are circles. We thus find the intensity of the ultrasonic absorption by the real squashing mode to be

$$I_M(\omega)\propto\frac{1}{\pi R^2}\int d^2r\,\delta(\omega-\omega(r))P_{2M}{}^2(\cos^2\gamma(\mathbf{r}))$$
$$=\frac{2r(\omega)}{R^2}\left|\frac{\partial\omega}{\partial r}\right|^{-1}_{r=r(\omega)}P_{2M}{}^2\left(\frac{\omega^2-\Omega_1{}^2}{c_2{}^2q^2}\right), \qquad (27)$$

where R is the radius of the cylinder.

The distribution of the vector $\hat{\mathbf{n}}$ in the rotating vessel must minimize the sum of the magnetic-anisotropy energy (5), the gradient energy, and the energy of the orienting effect of the vortex cores,

$$F_v=\frac{2}{5}a\lambda\int(\hat{z}_iR_{\alpha i}H_\alpha)^2\,d^2r \qquad (28)$$

and it must satisfy the boundary conditions[18,19]

$$\hat{\mathbf{n}}(R)=(5^{-1/2},\ (3/5)^{1/2},\ 5^{-1/2}). \qquad (29)$$

Here the dimensionless parameter λ is proportional to the angular rotation velocity of the vessel, i.e., to the density of vortex filaments, $n_v=2m\Omega/\pi\hbar$. The type of texture is determined by the relations among the parameters λ, n_v, and ξ_H. Typical experimental values are[19] angular velocities $\Omega\approx 1$–2 rad/s in fields $H=284$ (or 568) G, corresponding to the inequality $R\gg\xi_H\gg n^{1/2}_{-v}$. Two types of axisymmetric textures arise in this region, depending on the value of λ.

If $\lambda<1$ we have a so-called flare-out texture,[18] with the vector $\hat{\mathbf{n}}$ deviating slightly from the $\hat{\mathbf{z}}$ axis nearly throughout the volume of the cylinder, while at distances on the order of ξ_H from the walls it approaches the boundary value in (29):

$$\beta(r\to0)\approx\beta_1r, \qquad (30)$$

$$\cos\beta(r\to R)\approx5^{-1/2}+\beta_2(R-r). \qquad (31)$$

Here we have, for $R\gg\xi_H$,

$$\beta_1=c_1[2\pi R/(\xi_H^{eff})^3]^{1/2}\exp(-R/\xi_H^{eff}), \qquad (32)$$

$$\xi_H^{eff}=\xi_H'(1-\lambda)^{-1/2},\quad \beta_2\sim1/\xi_H \qquad (33)$$

(see Refs. 18 and 19), and $c_1\sim1$.

The maximum value of the frequency, $\Omega_2^2=\omega_M^2+c_1^2q^2+c_2^2q^2$, is reached at the axis of the vessel, while the minimum value, $\Omega_1^2=\omega_M^2+c_1^2q^2$, is reached at the surface of the cylinder. Since the minimum is degenerate, it corresponds to a square-root singularity in the spectral density. By analogy with the plane-geometry case, for the $M=0$ component we have

$$I_0(\omega\to\Omega_1)\propto\Omega_1{}^{1/2}/10^{1/2}c_2q(\omega-\Omega_1)^{1/2}\beta_2R, \qquad (34)$$

$$I_0(\omega\to\Omega_2)\propto8\omega/5R^2c_2{}^2q^2\beta_1{}^2. \qquad (35)$$

Since $I_0(\omega^2=(2\Omega_1^2+\Omega_2^2)/3)=0$, and β_1 is exponentially small, the ultrasonic absorption line corresponding to the $M=0$ component of the real squashing mode splits in two, as in the plane geometry. At the phase transition in the vortex cores, at which β_1 changes discontinuously,[19] $I_0(\omega\to\Omega_2)$ also changes discontinuously.

The lines corresponding to the components $M=\pm1$, ±1 do not undergo a texture-induced splitting. Their behavior near the corresponding minimum and maximum frequencies of the absorption spectra is

$$I_{\pm1}(\omega\to\Omega_1)\propto3(2\Omega_1)^{3/2}(\omega-\Omega_1)^{1/2}/5^{1/2}R(c_2q)^3\beta_2, \qquad (36)$$

$$I_{\pm1}(\omega\to\Omega_2)\propto24\Omega_2{}^2(\Omega_2-\omega)/5R^2(c_2q)^4\beta_1{}^2, \qquad (37)$$

$$I_{\pm2}(\omega\to\Omega_1)\propto3\Omega_1{}^{1/2}/40^{1/2}R|c_2|q(\omega-\Omega_1)^{1/2}\beta_2, \qquad (38)$$

$$I_{\pm2}(\omega\to\Omega_2)\propto12\Omega_2{}^3(\Omega_2-\omega)^2/5R^2(|c_2|q)^6\beta_1{}^2. \qquad (39)$$

The absorption intensity $I_{\pm1}$ reaches a maximum at $\omega=(\Omega_1\Omega_2)^{1/2}$.

The parameter λ increases with increasing angular velocity, and at values $\lambda>1$ the minimum of F_H+F_v corresponds to the value[20] $\cos\gamma=\lambda^{-1}$. For $\lambda>1$, we thus find a plateau in the texture of the vector $\hat{\mathbf{n}}$: Near the axis of the cylinder the angle β is approximately zero,

$$\beta(r\to0)\approx\beta_1r \qquad (40)$$

(here $\beta_1\sim1/\xi_H$). Further out, at a distance on the order of ξ_H from the axis, the angle β assumes a value of approximately

$$\sin^2\beta=4/5(1-\lambda^{-1})\equiv\sin^2\beta_0, \qquad (41)$$

and it retains this value all the way out to the surface layer, of thickness $\sim\xi_H$, near the walls of the vessel, where $\hat{\mathbf{n}}$ tends toward the boundary value in (29). The value of β is thus given by (41) almost everywhere in the vessel. The behavior of β near the inflection point r_0, where relation (41) is exact, can be described by

$$\beta(r\to r_0)=\beta_0+\beta_3(r-r_0)^3. \qquad (42)$$

The inflection point in the texture of the vector $\hat{\mathbf{n}}$ corresponds to a singularity in the ultrasonic absorption intensity corresponding to the components of the real squashing mode, described by

$$I_M(\omega\to\Omega_3)$$
$$\propto2r_0\lambda(2\Omega_3)^{1/3}P_{2M}{}^2(\lambda^{-2})/3R^2(c_2q)^{2/3}(5/2\beta_3\sin2\beta_0)^{1/3}|\omega-\Omega_3|^{2/3},$$
$$\Omega_3{}^2=\Omega_1{}^2+\lambda^{-2}c_2{}^2q^2. \qquad (43)$$

We thus find that as we go from the flare-out texture to the Gongadze-Gurgenishvili-Kharadze texture,[20] with $\lambda>1$, the ultrasonic absorption corresponding to all components of the real squashing mode has a singularity $|\omega-\Omega_3|^{-2/3}$ near $\omega=\Omega_3\lesssim\Omega_2$. The behavior of the absorption lines near $\omega=\Omega_1$, Ω_2 remains the same in form as for the flare-out texture [see (34)–(39)], except that here both β_1 and β_2 are on the order of $1/\xi_H$. The existence of two singularities, at $\omega=\Omega_1$ and $\omega=\Omega_2$, in the ultrasonic absorption at the $M=\pm2$ components will be observed as a splitting of the absorption lines corresponding to these modes, similar to the splitting of the $M=0$ line. In this texture we should thus observe an eightfold splitting of the absorption lines in a magnetic field: two lines for each of $M=0$ and ±2 and one line for each of $M=\pm1$.

Finally, in even stronger fields, at which the magnetic length becomes shorter than the distance between vortices (more precisely, under the condition[21] $\xi_H^2<\lambda/n_v$)—fields $H>10^3$ G for angular velocities $\Omega\sim1$ rad/s—there should be a transition to a spatially inhomogeneous texture of the vector $\hat{\mathbf{n}}$ (Ref. 21; this texture stands in contrast with the textures discussed above, which are essentially homogeneous through the volume of the vessel). In this texture, $\hat{\mathbf{n}}$ and correspondingly the angles β and γ vary periodically in space with the period of the unit cell per vortex. The behavior of the absorption intensity for all of the modes remains the same as in (34), (36), and (38) by virtue of the degenerate frequency minimum at the boundary of the vessel, i.e., as $\omega \to \Omega_1$. In addition, however, the frequency in (26), which is now a doubly periodic function of the point r, must in general have (according to the Morse theorem) at least one minimum, one maximum and two saddle points in each unit cell. Nondegenerate maxima and minima correspond to finite discontinuities in the spectral density, while the saddle points of the frequency,

$$\omega=\omega_c+\alpha_1(x-x_c)^2-\alpha_2(y-y_c)^2, \quad (44)$$

give rise to Van Hove logarithmic singularities[22] in the spectral density and thus in the ultrasonic absorption intensity for all components of the real squashing mode:

$$I_M(\omega\to\omega_c)\propto\frac{N}{\pi R^2}\frac{P_{2M}^2(\cos^2\gamma(r(\omega_c)))}{|\alpha_1\alpha_2|^{1/2}}\ln\frac{\Delta\omega}{|\omega-\omega_c|}. \quad (45)$$

Here N is the number of unit cells (vortices) in the vessel, and $\Delta\omega$ is of the order of the change in the frequency within one unit cell. The phase transition to the spatially inhomogeneous texture in a rotating cylinder with ^{3}He-B can thus be detected from the appearance of additional logarithmic singularities in the ultrasonic absorption intensity corresponding to the components of the real squashing mode.

This study was carried out during my visit at the Low Temperature Laboratory in Otaniemi, Finland, in June 1984. I wish to thank the staff of that Laboratory for their hospitality. I also wish to thank I. A. Fomin and M. Salomaa for useful discussions.

[1]K. J. Maki, J. Low Temp. Phys. **24**, 755 (1976).
[2]J. B. Ketterson, B. S. Shivaram, M. W. Meisel, *et al.*, in: Quantum Fluids and Solids (ed. E. D. Adams and G. G. Ihas), AIP Conference Proceedings, New York, 1983, p. 103.
[3]V. E. Koch and P. Wölfle, Phys. Rev. Lett. **46**, 486 (1981).
[4]O. Avenel, E. Varoquaux, and H. Ebisawa, Phys. Rev. Lett. **45**, 1952 (1980).
[5]L. Tewordt and N. Schopohl, J. Low Temp. Phys. **37**, 421 (1979).
[6]B. S. Shivaram, M. W. Meisel, B. K. Sarma, *et al.*, Phys. Rev. Lett. **49**, 1646 (1982).
[7]Yu. A. Vdovin, in: Primenenie metodov kvantovoĭ teorii polya k zadacham mnogikh tel (Application of the Methods of Quantum Field Theory to Many-Body Problems), Gosatomizdat, Moscow, 1963, p. 65 (Proceedings of the Moscow Engineering Physics Institute).
[8]K. Nagai, Progr. Theor. Phys. **54**, 1 (1975).
[9]L. Tewordt, D. Fay, P. Dörre, and D. Einzel, J. Low Temp. Phys. **21**, 645 (1975).
[10]P. Wölfle, Physica **90B**, 96 (1977).
[11]P. N. Brusov and V. N. Popov, Zh. Eksp. Teor. Fiz. **78**, 2419 (1980) [Sov. Phys. JETP **51**, 1217 (1980)].
[12]R. Combescot, J. Low Temp. Phys. **49**, 295 (1982).
[13]G. E. Volovik, Pis'ma Zh. Eksp. Teor. Fiz. **39**, 304 (1984) [JETP Lett. **39**, 365 (1984)].
[14]G. E. Volovik and M. V. Khazan, Zh. Eksp. Teor. Fiz. **87**, 483 (1984) [Sov. Phys. JETP **60**, 276 (1984)].
[15]D. D. Osheroff, Physica **90B**, 20 (1977).
[16]N. Schopohl and L. Tewordt, J. Low Temp. Phys. **45**, 67 (1981).
[17]H. Smith, W. F. Brinkman, and S. Engelsberg, Phys. Rev. **B15**, 199 (1977).
[18]P. J. Hakonen and G. E. Volovik, J. Phys. **c15**, L1277 (1982).
[19]P. J. Hakonen, O. T. Ikkala, S. T. Islander, *et al.*, J. Low Temp. Phys. **53**, 425 (1983).
[20]A. D. Gongadze, G. E. Gurgenishvili, and G. A. Kharadze, Fiz. Nizk. Temp. 7, 821 (1981) [Sov. J. Low Temp. Phys. 7, 397 (1981)].
[21]É. B. Sonin, Pis'ma Zh. Eksp. Teor. Fiz. **38**, 11 (1983) [JETP Lett. **38**, 11 (1983)].
[22]L. Van Hove, Phys. Rev. **89**, 1189 (1953).

Translated by Dave Parsons